Activation of the EGFR-PI3K-CaM Pathway by PRL-1 Ameliorates Liver Cirrhosis via ER Stress-dependent Calcium

Se Ho Kim
CHA University - Pocheon Campus: CHA University
Jae Yeon Kim
CHA University - Pocheon Campus: CHA University
Soo Young Park
CHA University - Pocheon Campus: CHA University
Won Tae Jeong
CHA University - Pocheon Campus: CHA University
Jin Man Kim
Seoul National University
Si Hyun Bae
Catholic University of Korea College of Medicine: Catholic University of Korea School of Medicine
Gi Jin Kim (gjkim@cha.ac.kr)
CHA University https://orcid.org/0000-0002-2320-7157

Research Article

Keywords: Calcium homeostasis, ER stress, Liver cirrhosis, Liver regeneration, mitochondria, Placenta-derived mesenchymal stem cells, Phosphatase of regenerating liver-1

Posted Date: July 15th, 2021

DOI: https://doi.org/10.21203/rs.3.rs-710155/v1

Abstract

Background: Accumulation of cholesterol and depletion of calcium induce hepatic injury through the endoplasmic reticulum (ER) stress response. ER stress regulates the calcium imbalance between the ER and mitochondria. Previously, we reported that phosphatase of regenerating liver-1 (PRL-1)-overexpressing placenta-derived mesenchymal stem cells (PD-MSCs^{PRL-1}) promoted liver regeneration through mitochondrial dynamics in a cirrhotic rat model. However, whether PRL-1 is involved in ER stress-dependent calcium is unclear. So, we demonstrated that PD-MSCs^{PRL-1} improves hepatic functions by regulating ER stress and calcium channels in a rat model of bile duct ligation (BDL).

Methods: Liver cirrhosis was induced in Sprague-Dawley (SD) rats using surgically induced BDL for 10 days. PD-MSCs and PD-MSCs^{PRL-1} ($2x10^6$ cells) were intravenously administered to animals, and their therapeutic effects were analyzed. WB-F344 cells exposed to thapsigargin (TG) were cocultured with PD-MSCs or PD-MSCs^{PRL-1}.

Results: ER stress markers (e.g., eIF2α, ATF4, and CHOP) were increased in the non-transplantation group (NTx) compared with the control group. PD-MSCs^{PRL-1} significantly decreased ER stress markers compared to NTx and induced dynamic changes in calcium channel markers (e.g., SERCA2b, IP3R, MCU, and VDAC1) (*$p<0.05$). In TG-treated WB-F344 cells, cocultivation with PD-MSCs^{PRL-1} decreased cytosolic CaM expression and cytosolic and mitochondrial Ca2+ concentrations; however, the ER Ca2+ concentration was increased compared to that in PD-MSCs (*$p<0.05$). Additionally, PRL-1 through epidermal growth factor receptor (EGFR) activated phosphatidylinositol-3-kinase (PI3K) signaling, resulting in calcium increases via CaM expression.

Conclusions: These findings suggest that PD-MSCs^{PRL-1} improved hepatic functions through calcium changes and attenuated ER stress in a BDL-injured rat model. Therefore, these results provide useful data for the development of next-generation MSC-based stem cell therapy for regenerative medicine in chronic liver disease.

Introduction

The endoplasmic reticulum (ER) is responsible for various cellular activities, such as protein secretion, synthesis, maturation, translation and folding in eukaryotic cells, and has an important role in regulating calcium concentration [1]. Because ER stress induces the accumulation of misfolded protein or depletion of calcium in the ER lumen, these events result in progression to severe stages of several diseases, such as diabetes, obesity, and nonalcoholic fatty liver disease (NAFLD)/nonalcoholic steatohepatitis (NASH) [2]. In particular, ER stress in liver fibrosis results in the accumulation of unfolded proteins, very low-density lipoprotein (VLDL), inflammatory cytokines and oxidative stress, and especially Ca2 + imbalances in the ER lumen [3]. Because calcium pump channels are dysregulated by ER stress in chronic liver diseases [4], calcium inflow controls sarco/endoplasmic reticulum Ca2 + ATPase (SERCA2b), and calcium release regulates inositol trisphosphate receptor (IP3R), ryanodine receptor 2 (RyR2) and calcium sensor

stromal interaction molecule 1 (STIM1) in the ER membrane [5]. In NAFLD, SERCA activity was impaired, leading to imbalanced calcium homeostasis under ER stress [6].

The unfolded protein response (UPR) and abnormal UPR pathway serve to restore normal functioning of the cell or cell death in case of irreversible disruption. Especially, PKR-like ER kinase (PERK), which is one of the key factors of the UPR, induces apoptosis by the transcription factor C/EBP homologous protein (CHOP) by phosphorylating eukaryotic translation initiation factor 2 alpha (eIF2α) to upregulate the expression of activating transcription factor 4 (ATF4). In addition, CHOP-deleted mice showed reduced apoptotic and necrotic hepatocyte death through decreases in the expression of alpha-smooth muscle actin (α-SMA) and transforming growth factor beta-1 (TGF-β1) [7]. However, the role of ER stress-dependent calcium influx in liver diseases including cirrhosis is still unknown.

Generally, Ca2 + signals in hepatocytes are generated by Ca2+-mobilizing growth factors through receptor tyrosine kinases (RTKs). RTKs are membrane proteins that bind to ligands such as growth factors, cytokines, and hormones in the plasma membrane. Several RTKs are expressed in the liver, including hepatocyte growth factor receptor (HGFR), vascular endothelial growth factor receptor (VEGFR), platelet-derived growth factor receptor (PDGF), and epidermal growth factor receptor (EGFR) [8]. In hepatic disease, EGFR is a key regulator in early inflammation and hepatocyte proliferation [9]. Activation of EGFR in liver disease affects liver regeneration through the downstream signaling pathway Ras-Raf-MEK-ERK1/2 and controls the phosphatidylinositol-3-kinase (PI3K)-Akt mechanism [10]. For activation of RTK-based signaling, several ligands bind to their specific receptors, leading to the activation of phospholipase C (PLC) or PI3K, which hydrolyzes phosphatidylinositol-4-5-bisphosphate (PIP2) to generate diacylglycerol (DAG) and inositol 1,4,5-trisphosphate (IP3). In chronic liver diseases, ER-resident IP3R calcium channels lead to elevated cytosolic and decreased ER calcium levels [11]. A previous report suggested that IGF-1 regulates spliced X-box binding protein 1 (sXBP-1) stability, protein synthesis and Ca2 + storage in the ER, thereby protecting beta cell ER stress-mediated cell death at the onset of type 1 and type 2 diabetes [12]. However, the RTKs that regulate Ca2 + signaling in cirrhotic rat liver are unknown.

Phosphatase of regenerating liver-1 (PRL-1) is a member of a small class of the prenylated PTP family and identified as an immediate early gene in the regenerating rat liver [13]. ALso, increased PRL-1 is involved in the regulation of proliferation and migration of mesenchymal stem cells in liver cirrhosis rat model [14] and shows high homology between humans and rats/mice [15]. Wang et al. and colleagues reported that PRL-1 localizes to the ER during the mitotic cell cycle [16]. During ER stress, increased PRL-1 suppressed apoptosis and enhanced ER function in a p53-dependent manner in injured cells [17]. In addition, the dual specificity tyrosine targeted by PRL-1 in the Ca2 + pathway has been reported [18]. However, research on PRL-1 directly modulating the Ca2 + pathway is lacking, and the binding of PRL-1 to RTK ligands in the plasma membrane is still unknown.

In previous reports, we demonstrated that placenta-derived MSC (PD-MSC) transplantation enhances hepatic function through increased antifibrotic effects, proliferation, and autophagy in a chronic liver

disease model [19]. Also, PRL-1-overexpressing PD-MSCs (PD-MSCs^{PRL-1}) enhanced hepatic functions by increasing mitochondrial functions and proliferative potential in a chronic liver disease model compared to naïve PD-MSCs [20]. However, whether PD-MSC^{PRL-1} transplantation is related to the ER stress mechanism induced by calcium in cirrhotic livers remains unclear. Therefore, the objective of this study was to investigate whether PD-MSC^{PRL-1} implantation induces Ca2 + influx in injured liver tissues in a rat model of bile duct ligation (BDL), whether it induces Ca2 + influx and how it correlates with ER stress. Finally, we evaluated the therapeutic mechanism by which PD-MSCs^{PRL-1} modulate ER stress-dependent calcium through RTK signaling in a rat model of BDL.

Materials & Methods

Cell culture

The collection of samples and their use for research purposes were approved by the institutional Review Board of CHA Bundang Hospital, Seoul, Republic of Korea (IRB 07–18). All participants provided written informed consent prior to sample collection. Placentas were extracted from women who were free of medical, obstetrical, and surgical complications and who delivered at term (≥ 37 gestational weeks). PD-MSCs were isolated as previously described [21] and cultured in α-modified minimal essential medium (α-MEM; HyClone Logan, UT, USA) supplemented with 10% fetal bovine serum (FBS; Gibco, Carlsbad, CA, USA), 1% penicillin/streptomycin (P/S; Gibco), 1 μg/mL heparin (Sigma-Aldrich, St. Louis, MO, USA), and 25 ng/mL human fibroblast growth factor-4 (hFGF-4; Peprotech, Inc., Rocky Hill, NJ, USA). The PRL-1 plasmid vector was purchased from Origene (#RG200435; Rockville, MD, USA). For overexpression of the PRL-1 gene, naïve PD-MSCs (passage = 7) were transfected using the AMAXA nucleofector system (Lonza, Basel, Switzerland) according to the manufacturer's instructions as previously described [20]. After transfection for 24 h, the cells were selected by 1.5 mg/mL neomycin. WB-F344 cells (rat liver epithelial cells) was cultured at 37°C in α-MEM supplemented with 10% FBS (Gibco) and 1% P/S (Gibco). All cells were maintained at 37°C in a 5% CO_2 incubator.

Animal models and transplantation of MSCs

Seven-week-old male Sprague-Dawley rats (Orient Bio, Inc., Seongnam, Republic of Korea) were maintained in an air-conditioned animal facility. Rats were anesthetized via intraperitoneal injection using avertin (2,2,2-tribromoethanol; Sigma-Aldrich) and underwent common BDL to induce liver cirrhosis as previously described [22]. Naïve PD-MSCs (PD-MSCs; n = 20) and PD-MSCs^{PRL-1} (PD-MSCs^{PRL-1}; n = 20) were stained with the PKH67 Fluorescent Cell Linker Kit (Sigma-Aldrich) and injected intravenously through the tail vein (2x10^6 cells/animal) in the transplantation group. Nontransplanted rats (NTx; n = 20) and sham control rats (Con; n = 5) were maintained. The rats were sacrificed after 1, 2, 3, and 5 weeks to extract their liver tissues and blood samples. The experimental processes and protocols for animal modeling were approved by the Institutional Animal Care Use Committee of CHA University, Seongnam, Republic of Korea (IACUC-200033).

Liver histology and serum biochemistry

Liver tissue samples were fixed in 10% neutral buffered formalin (NBF), embedded in paraffin, and sectioned at 5 μm thick for hematoxylin and eosin (H&E) and Sirius red staining. Representative images of whole sections of the liver were captured and quantified using a digital slide scanner (3DHISTECH, Ltd., Budapest, Hungary). The serum concentrations of ALT, AST, TBIL, and ALB were measured from individual blood samples (Southeast Medi-Chem Institute, Busan, Republic of Korea).

Immunofluorescence

For analysis of gene expression in liver tissues, samples were sectioned at 6 μm thickness and fixed with 4% paraformaldehyde. The liver tissues from each group were blocked using Protein Block Serum-Free solution (Dako, Santa Clara, CA, USA) for 1 h. The primary antibody was used as follows: SERCA2b (1:1000; Invitrogen, Carlsbad, CA, USA). The sections were stained with 4',6-diamidino-2-phenylindole (DAPI; Invitrogen) and observed by confocal microscopy (LSM 700). Representative images were analyzed by ZEN blue software (Zeiss). The experiment was performed in at least duplicate.

Immunohistochemistry

For determination of the expression of calcium channels in the ER, liver tissues from each group were sectioned at a thickness of 5 μm and fixed with 10% NBF. The fixed tissues were reacted in 3% hydrogen peroxide (H_2O_2) in 100% methanol to block endogenous peroxidase enzyme. The following antibodies were used: CHOP (1:50; Santa Cruz, Dallas, TX, USA), anti-calmodulin (1:100; Novus Biologicals, Littleton, CO, USA) and anti-PCNA (1:500; company). CHOP was performed using Proteinase K (20 μg/mL) (Dako) instead of antigen retrieval. However, anti-calmodulin and anti-PCNA antibodies were used for antigen retrieval before incubation at 4 ℃ overnight. Incubation with horseradish peroxidase-conjugated streptavidin–biotin complex (Dako) and 3,3-diaminobenzidine (EnVision Systems, Santa Clara, CA, USA) was performed to generate a chromatic signal. For counterstaining, Mayer's hematoxylin (Dako) was used. Representative images were captured and quantified using a digital slide scanner (3DHISTECH, Ltd.).

Quantitative real-time PCR

Total RNA was isolated from samples with TRIzol (Invitrogen). cDNA was synthesized using Superscript III reverse transcription (Invitrogen) according to the manufacturer's instructions. For determination of the expression of calcium channel factors in liver tissues and hepatocytes, qRT-PCR was conducted with rat primers (Supplementary Table 1, designed by BIONEER, Daejeon, Korea) and SYBR Green Master Mix (Roche, Basel, Switzerland) using the CFX Connect™ Real Time System (Bio-Rad, Hercules, CA, USA). Rat GAPDH was used as an internal control for normalization, and each sample was analyzed in duplicate.

Western blotting

Homogenized liver tissues and samples were lysed with RIPA buffer containing protease inhibitor cocktail (Roche) and phosphatase inhibitor (Sigma-Aldrich). Quantified 40 μg of protein extraction was loaded in

6 ~ 15% sodium dodecyl sulfate polyacrylamide gel electrophoresis (SDS-PAGE). The separated proteins were transferred to polyvinylidene difluoride (PVDF) membranes (Bio-Rad). The following primary antibodies were used: anti-SERCA2b (1:500; Invitrogen), anti-MCU (1:1000; Invitrogen), anti-IP3R (1:800; Cell Signaling Technology), anti-VDAC1, anti-total-eIF2α, anti-phospho-eIF2α, anti-ATF4, anti-CHOP, anti-PI3K-p110α (1:1000; all from Cell Signaling Technology), anti-PI3K-p85 (1:3000; BD Biosciences, San Jose, CA, USA), anti-PERK (1:200; Santa Cruz), anti-GRP75 (1:500; Abcam), and anti-calmodulin (1:500; Novus Biologicals). The loading control was anti-GAPDH (1:2000; AbFrontier, Seoul, Republic of Korea). After the membranes were washed, the following secondary antibodies were used: anti-mouse IgG and anti-rabbit IgG (1:8,000; all from Bio-Rad). The protein bands were detected using a Clarity Western ECL kit (Bio-Rad) and detected with a ChemiDoc imaging system (Bio-Rad).

Calcium influx using a fluorescence resonance energy transfer (FRET) biosensor

For confirmation of calcium influx in hepatocytes, cytoplasm-targeting CMV-Y-GECO1, ER-targeting CMV-ER-LAR-GECO1, and mitochondria-targeting CMV-mito-GEM-GECO1 were purchased (Addgene, Watertown, MA, USA). Cells were transfected using Lipofectamine 2000 (Thermo Fisher Scientific) for 4 h and treated with TG (500 nM) for 24 h. For simultaneous monitoring of the Ca2 + concentration in the ER, cytoplasm, and mitochondria, widefield imaging was performed with a confocal microscope (LSM880; Carl Zeiss) at 37°C in a humidified atmosphere with 5% CO_2.

Phospho-RTK proteome profiler array

For analysis of the interaction of PRL-1 and RTKs, a human phospho-RTK Array kit (R&D Systems, Minneapolis, USA) was used following the manufacturer's assay procedures. Briefly, cell lysates ($1x10^7$ cells) were diluted and incubated overnight with anti-phospho-tyrosine-HRP detection antibody. Captured signals represent the amount of phosphorylated protein.

Statistical analysis

All experiments were performed in at least duplicate or triplicate. The results are presented as the mean ± standard deviation (SD). Student's t-test was performed for groupwise comparisons, and a *p*-value less than 0.05 was considered statistically significant. One-way ANOVA was performed using pairwise comparisons and multiple paired t-tests.

Results

PD-MSCs^{PRL-1} decreased ER stress in a rat model of BDL and in hepatocytes

In the UPR pathway, PERK-eIF2α-ATF4-CHOP signaling is implicated in liver diseases [23]. To analyze UPR pathway activation by PD-MSC^{PRL-1} transplantation, we assessed the expression of CHOP, which is an ER stress-mediated transcription factor, in liver tissues using immunohistochemistry (IHC). The expression of CHOP in the nuclei of hepatocytes was significantly increased in the BDL-induced nontransplantation

(NTx) group compared to the normal control (Con) group (*p < 0.05). Interestingly, the CHOP level was reduced, and CHOP translocation into the nucleus was significantly decreased in PD-MSCs^{PRL-1} (Fig. 1a and Supplementary Fig. 1a, *p < 0.05). In the NTx group, phosphorylated eIF2α (p-eIF2α) expression was increased at 1 and 2 weeks; however, the expression of PERK, ATF4 and CHOP decreased.

In contrast, the transplantation groups (Tx) showed decreased levels compared to the NTx group. Especially, the expression of PERK and p-eIF2α was significantly reduced in the PD-MSC^{PRL-1} group (Fig. 1b-e, *p < 0.05). Thapsigargin (TG) is an inhibitor of SERCA2b in hepatocyte-specific calcium channels on the ER membrane, resulting in cellular apoptosis (Fig. 1f). To induce ER stress in hepatocytes, we analyzed the expression of ER stress markers after 500 nM TG treatment for 24 h regardless of PD-MSC and PD-MSC^{PRL-1} cocultivation (Fig. 1g). The protein levels of ER stress markers in the WB-F344 cells treated with TG were substantially increased. However, their expression levels were significantly decreased after PD-MSC cocultivation. Specifically, PD-MSC^{PRL-1} cocultivation resulted in significantly reduced expression compared to that of naïve PD-MSCs (Fig. 1h and i, *p < 0.05). These findings indicated that PD-MSCs^{PRL-1} more efficiently decreased ER stress than naïve PD-MSCs in cirrhotic rat livers and hepatocytes.

PD-MSCs^{PRL-1} regulated calcium channels in a rat model of BDL and in hepatocytes

A calcium imbalance between the ER and mitochondria in the liver leads to the development of chronic metabolic diseases and impaired organelle function [24]. So, we confirmed the expression levels of calcium channels in the ER membrane (e.g., SERCA2b and IP3R) and mitochondria (e.g., VDAC1 and MCU) as well as ER-mitochondrial Ca2 + transfer factors (e.g., GRP75) in a rat model of BDL by Western blotting (Fig. 2a). The expression levels of SERCA2b, IP3R, and GRP75 were increased in the NTx group compared to the normal group. In contrast, all Tx groups showed decreased levels compared with the NTx group. In the PD-MSC^{PRL-1} group, the GRP75 levels were significantly decreased at 1 and 3 weeks (Fig. 2b-e, *p < 0.05). However, IP3R and GRP75 expression in the PD-MSC^{PRL-1} group was dramatically increased compared with that in the PD-MSC group (Supplementary Fig. 2a and b). Interestingly, the mRNA and protein levels of VDAC1 and MCU were increased in the PD-MSC^{PRL-1} Tx group (Fig. 2e and f, Supplementary Fig. 2c and d, *p < 0.05). Additionally, TG treatment induced a decrease in the expression levels of IP3R, VDAC1, and MCU, whereas the expression levels of GRP75 and CaM were increased in the WB-F344 hepatocyte cell line. With PD-MSC^{PRL-1} cocultivation, the expression levels of IP3R, VDAC1, MCU, and GRP75 were significantly changed compared to those with naïve PD-MSCs, although no significant change was found in the mRNA level between the treated group and the cocultivation group (Supplementary Fig. 2e-i, *p < 0.05). However, the CaM levels were decreased (Fig. 2g and h). Also, we confirmed the degree of colocalization with SERCA2b and ER Tracker by immunofluorescence (IF) staining (Fig. 2i). The expression of SERCA2b in the NTx group was increased; however, the expression was significantly decreased in the PD-MSC^{PRL-1} group compared to the NTx group and the PD-MSC group (Fig. 2j, *p < 0.05). These results indicated that PD-MSCs^{PRL-1} efficiently regulate calcium channels between the ER and mitochondria in cirrhotic rat livers and hepatocytes.

PD-MSCs^{PRL-1} regulate calcium influx in rat hepatocytes

To further analyze the concentration of calcium in hepatocytes, we confirmed the mRNA and protein levels of SERCA2b by qRT-PCR and Western blotting, respectively. Their mRNA expression levels were increased in the TG-treated group compared to the normal group but decreased in the cocultivation group (Fig. 3a). Although the protein expression was reduced after TG treatment, the expression of SERCA2b was significantly increased in cocultivated PD-MSCs and PD-MSCs^{PRL-1} (Fig. 3b and c, *p < 0.05). In particular, the mRNA expression of SERCA2b and STIM1, which are calcium sensors in the ER, was significantly increased in the PD-MSCs^{PRL-1} (Supplementary Fig. 3a and b). To investigate the change in calcium in the ER, cytoplasm, and mitochondria of hepatocytes, we analyzed these organelles using calcium biosensors, including ER-LAR-GECO for the ER, Y-GECO1 for the cytoplasm, and mito-GEM-GECO1 for the mitochondria (Fig. 3d). The influx of ER Ca2 + in the TG-treated WB-F344 cells declined, whereas the influx of cytoplasmic and mitochondrial Ca2 + was enhanced. Interestingly, PD-MSC^{PRL-1} cocultivation induced an enhanced ER Ca2 + concentration while decreasing the influx of cytoplasmic and mitochondrial Ca2 + compared to that of PD-MSCs (Fig. 3e-g, *p < 0.05). These results indicated that PD-MSC^{PRL-1} cocultivation modulates calcium influx in ER stress-induced hepatocytes.

PRL-1 regulates EGFR-PI3K-CaM calcium signaling in the BDL-injured rat liver

To further investigate calcium signaling by PRL-1, we analyzed the expression of EGFR in hepatocytes injured by pentamidine regardless of cocultivation and recombinant PRL-1 treatment. As shown in Fig. 4a, PRL-1 binds to EGFR and activates PI3K-p110α expression. PIP2 is split into IP3, and released IP3 binds to IP3R on the ER membrane. These signaling pathways release Ca2 + and regulate the cellular response via the Ca2+/CaM complex (Fig. 4a). We performed an RTK dot blot assay and identified which RTK was phosphorylated among 49 different RTKs (Fig. 4b). Compared to PD-MSCs, PD-MSCs^{PRL-1} strongly activated phosphorylated EGFR after recombinant PRL-1 treatment. In addition, recombinant PRL-1 and pentamidine inhibition treatment reduced the activity of phosphorylated EGFR (Fig. 4c, *p < 0.05). The expression of PI3K, which is a downstream factor of EGFR through PRL-1, was increased in the PD-MSC^{PRL-1} group compared to the NTx and PD-MSC groups, whereas the CaM levels were strongly decreased at 1, 3, and 5 weeks (Fig. 4e and f, *p < 0.05). Additionally, endogenous CaM levels in cirrhotic livers in the NTx group were significantly increased; however, their expression levels were significantly reduced in the PD-MSC^{PRL-1} group compared to the naïve PD-MSC group (Fig. 4g and h, *p < 0.05). These results suggest that PRL-1 interacts with EGFR-PI3K-CaM and regulates calcium levels in BDL-injured rat livers.

Hepatic regenerative effects of PD-MSCs^{PRL-1} in a rat model of BDL

Previously, we reported that administration of PD-MSCs^{PRL-1} improved hepatic functions in a rat model of BDL [20]. In the NTx group, the collagen accumulation in liver tissues was significantly increased compared to that in the normal group. However, the amount of Sirius red-positive areas significantly declined in all Tx groups. In particular, antifibrotic effects due to decreased collagen deposition were

dramatically observed in the PD-MSC^{PRL-1} group compared to the PD-MSC group (Fig. 5a and b, *p < 0.05). In the blood chemistry analysis, the levels of alanine aminotransferase (ALT), aspartate aminotransferase (AST), and total bilirubin (TBIL) were decreased in the transplantation groups compared to the NTx group, whereas the albumin (ALB) level was significantly increased (Fig. 5c-f, *p < 0.05). In particular, the PD-MSC^{PRL-1} group exhibited substantially decreased ALT and AST and increased ALB levels. To further confirm the proliferation of hepatocytes in the livers of BDL-induced rats by transplantation, we examined proliferating cell nuclear antigen (PCNA) by IHC (Fig. 5g). Compared to that of naïve PD-MSCs, the positive signal was significantly enhanced in the PD-MSC^{PRL-1} groups (Fig. 5h, *p < 0.05). Additionally, the expression of hepatic ALB and proliferation markers (e.g., CDK4 and cyclin D1) in the PD-MSC^{PRL-1} group was remarkably higher than that in the PD-MSC group (Fig. 5i). The correlation coefficient between ALB and cyclin D1 expression was $R^2 = 0.8819$ (Fig. 5j). These results suggest that PD-MSCs^{PRL-1} promote hepatic regeneration in a BDL-injured rat model.

Discussion

Abnormal calcium levels lead to the ER stress response, contributing to hepatic lipid accumulation and apoptosis in chronic liver disease [25]. This ER stress response is perturbed due to the accumulation of unfolded/misfolded proteins by calcium depletion [26]. The PERK-eIF2α-ATF4 axis mediates pharmacologic ER stress-induced hepatosteatosis, resulting from lipid homeostasis in several pathways [27]. Therefore, PERK deficiency and increased reactive oxygen species (ROS) due to accumulated lipids and protein aggregation induce apoptosis in response to ER stress as well as eIF2α phosphorylation [1]. In mice with liver-specific ATF4 knockout, hepatic steatosis was stimulated by AMPK inhibition and triglyceride accumulation [28]. In addition, increased phosphorylated PERK and CHOP levels induce intracellular Ca2 + overload by upregulating Bax expression and increasing the active form of caspase-3 [29]. Therefore, persistent ER stress causes several degenerative diseases, including liver diseases associated with steatosis, through cell death [1]. Recently, many scientists have reported the efficacies of MSCs on chronic diseases such as diabetic lung fibrosis, hepatic steatosis and chromium intoxication by decreasing ER stress [30]. MSCs reduced the ER stress response by decreasing XBP1 and Bip expression via the PERK-Nrf2 signaling pathway [31]. Based on this evidence, our study focused on whether PRL-1 overexpressing PD-MSCs transplatnation can suppress ER stress-dependent calcium influx in liver of a cirrhosis rat model induced by BDL and if they have a positive effect which mechanisms is involved.

In CHOP knockout mice following BDL-induced cholestasis, the expression of α-SMA and transforming growth factor 1 and apoptotic and necrotic hepatocytes were decreased, resulting in an ER stress response. Therefore, an increased ER stress response induced the overexpression of CHOP in bile acid-induced hepatocytes through PERK-eIF2α-ATF4 signaling [7]. In high fat diet (HFD)-induced rats with NAFLD, rat BM-MSC transplantation alleviated ATF4 and CHOP expression [32]. Additionally, MSC treatment in palmitic acid-induced hepatocytes reduced CHOP expression, whereas SERCA2b silencing reversed the ER stress response and calcium homeostasis [33]. These data are similar to our data showing that CHOP expression and PERK-eIF2α-ATF4 signaling were increased in the BDL-injured rat

model (Fig. 1). Furthermore, we observed changes in calcium channel factors in ER membranes (e.g., SERCA2b and IP3R) and mitochondrial membranes (e.g., VDAC1 and MCU) in the BDL-induced rat livers. Following PD-MSC or PD-MSC^{PRL-1} transplantation, the levels of ER stress-related markers and calcium channel markers were dramatically reduced in a rat model of BDL. Treatment of hepatocytes with TG, which is a SERCA inhibitor, induced calcium depletion in the ER and then the ER stress response by enhancing the PERK-eIF2α-ATF4-CHOP axis and calcium channel markers in mitochondria. Compared to naïve PD-MSCs, PD-MSCs^{PRL-1} resulted in dramatic changes in ER Ca2 + transport factors in vivo and in vitro (Figs. 1, 2, 3). These results could indicate that activated nonparenchymal cells (e.g., Kupffer cells and hepatic stellate cells) and parenchymal cells (e.g., hepatocytes) in a chronic liver disease model are different in terms of the ER stress response and cell death injury [34]. In activated LX2 cells, GRP78 knockdown alleviated ER stress and restored intracellular calcium levels through overexpression of SERCA2 [35]. Many reports have indicated that treatment of hepatocytes with several bile acids increases the expression of ER stress-related genes (e.g., Bip, XBP1 and CHOP), calcium release and mitochondrial oxidative stress [36]. Also, glucose-regulated protein (GRP78) and X-box binding protein 1 (XBP1) are activated by bile acid accumulation [37].

In the present study, we confirmed a significant difference in the expression of PD-MSCs^{PRL-1} compared to naïve PD-MSCs when they were treated with 100 μM LCA and cocultivated with WB-F344 cells. However, in contrast to previous results, the expression pattern was similar to that after treatment with TG and LCA in WB-F344 (Supplementary Figs. 5, 6). In TG-treated hepatocytes, calcium influx was analyzed using a genetically encoded Ca2 + biosensor in the ER, mitochondria, and cytoplasm. PD-MSC^{PRL-1} cocultivation resulted in dynamic changes and recovered calcium levels in the ER (Fig. 3). However, hepatocyte-specific calcium channels in the ER and mitochondria need to be further confirmed for isolation from the ER and mitochondria in hepatocytes. Our previous reports demonstrated that function-enhanced PD-MSCs^{PRL-1} were generated [38] and that transplantation improved mitochondrial biogenesis and liver function in a BDL-injured rat model [20]. Additionally, PD-MSCs^{PRL-1} promoted antiadipogenic effects via improved IGFBP expression in orbital fibroblasts [39]. Accumulating evidence suggests that excessive intracellular lipids lead to deleterious ER stress and mitochondrial oxidative stress in hepatocytes [40].

Interestingly, we found that PD-MSCs^{PRL-1} reduce ER stress via PERK-ATF4-CHOP signals in the BDL-injured rat model and regulate the calcium imbalance between the ER and mitochondria, resulting in improvements in hepatic function. PERK-dependent eIF2α expression reduced the synthesis of cyclin D1 in stressed cells [41]. To further analyze the changes in calcium channels induced by PRL-1, we performed recombinant PRL-1 treatment and found it increased IP3R, VDAC1, MCU, and GRP75 expression in LCA-induced hepatocytes (Supplementary Figure S7). Additionally, we found that PD-MSC^{PRL-1} transplantation improved CDK4 and cyclin D1 expression, leading to increased proliferation of hepatocytes compared to that with PD-MSCs (Fig. 5). These data are consistent with Suzuki et al., and their colleagues reported that PRL-1 inhibits apoptosis with transactivation domains of the p53 transcriptional activator [17]. Upon the ER stress response, this molecules is localized to the ER in a cell

cycle-dependent manner, modulating mitosis [16]. In addition, PTPs, including PRL-1, contribute to calcium influx. PTPs are responsible for dephosphorylating EGFR, indicating a similar specific activity as its Ser/Thr phosphatase activity [42]. Activated EGFR generates Ca2 + signals and subsequently controls the Ca2+/CaM complex [43]. Based on this evidence, we hypothesized that PRL-1 may bind to the first signaling RTKs and affect intracellular calcium levels. Activated EGFR regulates ER stress-dependent calcium signaling, which activates phospholipase C gamma (PLCγ) and the MAPK pathway [44]. We confirmed that phosphorylated EGFR expression was upregulated by recombinant PRL-1 or PD-MSCs^{PRL-1} and activated the expression of the downstream factor PI3K-p110α, but not PI3K-p85, in the PD-MSC^{PRL-1} groups (Fig. 4, Supplementary Figure S4); furthermore, PD-MSC^{PRL-1} transplantation suppressed CaM expression in hepatocytes, resulting in decreased ER stress and calcium pathway activation. However, the fundamental mechanism between PRL-1 and EGFR needs requires study.

Conclusion

In conclusion, administration of PD-MSCs^{PRL-1} decreased ER stress and modulated calcium levels through the EGFR-PI3K-CaM signaling pathway, leading to improved hepatic functions in a rat model of BDL. Therefore, our data for understanding of this therapeutic mechanism provides useful data for the development of next-generation MSC-based stem cell therapy for regenerative medicine in chronic liver disease.

Abbreviations

ALT: alanine aminotransferase; ALB: albumin; α-MEM: Alpha-modified minimal essential medium; AST: aspartate aminotransferase; ATF4: activating transcription factor 4; BDL: Bile duct ligation; CaM: Calmodulin; CDK4: cyclin-dependent kinase 4; CHOP: C/EBP homologous protein; DAPI: 4',6-diamidino-2-phenylindole; EGFR: epidermal growth factor receptor; FBS: Fetal bovine serum; GAPDH: Glyceraldehyde 3-phosphate dehydrogenase; GFP: Green fluorescent protein; GRP75: glucose regulated protein 75; hFGF-4: Human fibroblast growth factor-4; H&E: Hematoxylin & eosin; IP3R: inositol trisphosphate receptor; LCA: lithocholic acid; MCU: mitochondria calcium uniporter; NBF: neutral buffered formalin; NTx: nontransplantation; PERK: PKR-like ER kinase; PCNA: proliferating cell nuclear antigen; PD-MSCs: Placenta-derived mesenchymal stem cells; p-eIF2α: phosphorylated eIF2 alpha; PI3K, phosphatidylinositol-3-kinase; PRL-1: Phosphatase of regenerating liver-1; P/S: Penicillin/streptomycin; RTK, receptor tyrosine kinases; SERCA2b: sarco/endoplasmic reticulum Ca2+ ATPase; SD: Sprague-Dawley; STIM1: stromal interaction molecule 1; TBIL: total bilirubin; TG: thapsigargin; VDAC1, voltage dependent anion channel 1

Declarations

Acknowledgments

We thank Ho Jeong Kim (Incheon Catholic University) for helping us with the graphical abstract.

Authors' contributions

SHK and JYK did analysis and interpretation of data, and manuscript drafting. SHK, JYK, WTJ did animal model construction, validation and formal analysis. SHK, JYK, SYP helped critical comments. JMK and SHB did project administration, and funding acquisition. GJK conceived and designed the experiments, and contributed to the manuscript drafting and final approval of manuscript. All authors have read and agreed to the published version of the manuscript.

Funding

This research was supported by a grant of the Korea Health Technology R&D Project through the Korea Health Industry Development Institute (KHIDI), funded by the Ministry of Health & Welfare, Republic of Korea (HI17C1050) and Basic Science Research Program through the National Research Foundation of Korea (NRF) funded by the Ministry of Education, Science and Technology (2020M3A9B302618221).

Availability of data and materials

The data that support the findings of this study are available from the corresponding author upon reasonable request.

Ethics approval and consent to participate

The collection of samples and their use for research purposes were approved by the institutional Review Board of CHA Bundang Hospital, Seoul, Republic of Korea (IRB 07-18). All participants provided written informed consent prior to sample collection. The experimental processes and protocols for animal modeling were approved by the Institutional Animal Care Use Committee of CHA University, Seongnam, Republic of Korea (IACUC-200033).

Consent for publication

Not applicable.

Competing interests

The authors declare that there has no conflict of interest.

References

1. Malhi H, Kaufman RJ. Endoplasmic reticulum stress in liver disease. J Hepatol. 2011;54(4):795-809.
2. Di Conza G, Ho PC. ER Stress Responses: An Emerging Modulator for Innate Immunity. Cells. 2020;9(3).
3. Maiers JL, Malhi H. Endoplasmic Reticulum Stress in Metabolic Liver Diseases and Hepatic Fibrosis. Semin Liver Dis. 2019;39(2):235-48.

4. Kao E, Shinohara M, Feng M, Lau MY, Ji C. Human immunodeficiency virus protease inhibitors modulate Ca2+ homeostasis and potentiate alcoholic stress and injury in mice and primary mouse and human hepatocytes. Hepatology. 2012;56(2):594-604.
5. Jousset H, Frieden M, Demaurex N. STIM1 knockdown reveals that store-operated Ca2+ channels located close to sarco/endoplasmic Ca2+ ATPases (SERCA) pumps silently refill the endoplasmic reticulum. J Biol Chem. 2007;282(15):11456-64.
6. Ni HM, Baty CJ, Li N, Ding WX, Gao W, Li M, Chen X, Ma J, Michalopoulos GK, Yin XM. Bid agonist regulates murine hepatocyte proliferation by controlling endoplasmic reticulum calcium homeostasis. Hepatology. 2010;52(1):338-48.
7. Tamaki N, Hatano E, Taura K, Tada M, Kodama Y, Nitta T, Iwaisako K, Seo S, Nakajima A, Ikai I, Uemoto S. CHOP deficiency attenuates cholestasis-induced liver fibrosis by reduction of hepatocyte injury. Am J Physiol Gastrointest Liver Physiol. 2008;294(2):G498-505.
8. Lemmon MA, Schlessinger J. Cell signaling by receptor tyrosine kinases. Cell. 2010;141(7):1117-34.
9. Berasain C, Avila MA. The EGFR signalling system in the liver: from hepatoprotection to hepatocarcinogenesis. J Gastroenterol. 2014;49(1):9-23.
10. Komposch K, Sibilia M. EGFR Signaling in Liver Diseases. Int J Mol Sci. 2015;17(1).
11. Wang Y, Li G, Goode J, Paz JC, Ouyang K, Screaton R, Fischer WH, Chen J, Tabas I, Montminy M. Inositol-1,4,5-trisphosphate receptor regulates hepatic gluconeogenesis in fasting and diabetes. Nature. 2012;485(7396):128-32.
12. Ozcan U, Cao Q, Yilmaz E, Lee AH, Iwakoshi NN, Ozdelen E, Tuncman G, Gorgun C, Glimcher LH, Hotamisligil GS. Endoplasmic reticulum stress links obesity, insulin action, and type 2 diabetes. Science. 2004;306(5695):457-61.
13. Wei M, Korotkov KV, Blackburn JS. Targeting phosphatases of regenerating liver (PRLs) in cancer. Pharmacol Ther. 2018;190:128-38.
14. Kim JY, Jun JH, Park SY, Yang SW, Bae SH, Kim GJ. Dynamic Regulation of miRNA Expression by Functionally Enhanced Placental Mesenchymal Stem Cells PromotesHepatic Regeneration in a Rat Model with Bile Duct Ligation. Int J Mol Sci. 2019;20(21).
15. Boverhof DR, Burgoon LD, Tashiro C, Sharratt B, Chittim B, Harkema JR, Mendrick DL, Zacharewski TR. Comparative toxicogenomic analysis of the hepatotoxic effects of TCDD in Sprague Dawley rats and C57BL/6 mice. Toxicol Sci. 2006;94(2):398-416.
16. Wang J, Kirby CE, Herbst R. The tyrosine phosphatase PRL-1 localizes to the endoplasmic reticulum and the mitotic spindle and is required for normal mitosis. J Biol Chem. 2002;277(48):46659-68.
17. Suzuki S, Tsutsumi S, Chen Y, Ozeki C, Okabe A, Kawase T, Aburatani H, Ohki R. Identification and characterization of the binding sequences and target genes of p53 lacking the 1st transactivation domain. Cancer Sci. 2020;111(2):451-66.
18. He J, Yao J, Sheng H, Zhu J. Involvement of the dual-specificity tyrosine phosphorylation-regulated kinase 1A-alternative splicing factor-calcium/calmodulin-dependent protein kinase IIdelta signaling pathway in myocardial infarction-induced heart failure of rats. J Card Fail. 2015;21(9):751-60.

19. Jung J, Choi JH, Lee Y, Park JW, Oh IH, Hwang SG, Kim KS, Kim GJ. Human placenta-derived mesenchymal stem cells promote hepatic regeneration in CCl4 -injured rat liver model via increased autophagic mechanism. Stem Cells. 2013;31(8):1584-96.
20. Kim JY, Choi JH, Jun JH, Park S, Jung J, Bae SH, Kim GJ. Enhanced PRL-1 expression in placenta-derived mesenchymal stem cells accelerates hepatic function via mitochondrial dynamics in a cirrhotic rat model. Stem Cell Res Ther. 2020;11(1):512.
21. Lee MJ, Jung J, Na KH, Moon JS, Lee HJ, Kim JH, Kim GI, Kwon SW, Hwang SG, Kim GJ. Anti-fibrotic effect of chorionic plate-derived mesenchymal stem cells isolated from human placenta in a rat model of CCl(4)-injured liver: potential application to the treatment of hepatic diseases. J Cell Biochem. 2010;111(6):1453-63.
22. Kountouras J, Billing BH, Scheuer PJ. Prolonged bile duct obstruction: a new experimental model for cirrhosis in the rat. Br J Exp Pathol. 1984;65(3):305-11.
23. Li D, Wang WJ, Wang YZ, Wang YB, Li YL. Lobaplatin promotes (125)I-induced apoptosis and inhibition of proliferation in hepatocellular carcinoma by upregulating PERK-eIF2alpha-ATF4-CHOP pathway. Cell Death Dis. 2019;10(10):744.
24. Arruda AP, Pers BM, Parlakgul G, Guney E, Inouye K, Hotamisligil GS. Chronic enrichment of hepatic endoplasmic reticulum-mitochondria contact leads to mitochondrial dysfunction in obesity. Nat Med. 2014;20(12):1427-35.
25. Ali ES, Petrovsky N. Calcium Signaling As a Therapeutic Target for Liver Steatosis. Trends Endocrinol Metab. 2019;30(4):270-81.
26. Bahar E, Kim H, Yoon H. ER Stress-Mediated Signaling: Action Potential and Ca(2+) as Key Players. Int J Mol Sci. 2016;17(9).
27. Jo H, Choe SS, Shin KC, Jang H, Lee JH, Seong JK, Back SH, Kim JB. Endoplasmic reticulum stress induces hepatic steatosis via increased expression of the hepatic very low-density lipoprotein receptor. Hepatology. 2013;57(4):1366-77.
28. Li K, Xiao Y, Yu J, Xia T, Liu B, Guo Y, Deng J, Chen S, Wang C, Guo F. Liver-specific Gene Inactivation of the Transcription Factor ATF4 Alleviates Alcoholic Liver Steatosis in Mice. J Biol Chem. 2016;291(35):18536-46.
29. Wang X, Zhuang Y, Fang Y, Cao H, Zhang C, Xing C, Guo X, Li G, Liu P, Hu G, Yang F. Endoplasmic reticulum stress aggravates copper-induced apoptosis via the PERK/ATF4/CHOP signaling pathway in duck renal tubular epithelial cells. Environ Pollut. 2021;272:115981.
30. Chen Y, Zhang F, Wang D, Li L, Si H, Wang C, Liu J, Chen Y, Cheng J, Lu Y. Mesenchymal Stem Cells Attenuate Diabetic Lung Fibrosis via Adjusting Sirt3-Mediated Stress Responses in Rats. Oxid Med Cell Longev. 2020;2020:8076105.
31. Lee EJ, Cardenes N, Alvarez D, Sellares J, Sembrat J, Aranda P, Peng Y, Bullock J, Nouraie SM, Mora AL, Rojas M. Mesenchymal stem cells reduce ER stress via PERK-Nrf2 pathway in an aged mouse model. Respirology. 2020;25(4):417-26.

32. Ulum B, Teker HT, Sarikaya A, Balta G, Kuskonmaz B, Uckan-Cetinkaya D, Aerts-Kaya F. Bone marrow mesenchymal stem cell donors with a high body mass index display elevated endoplasmic reticulum stress and are functionally impaired. J Cell Physiol. 2018;233(11):8429-36.
33. Li L, Zeng X, Liu Z, Chen X, Li L, Luo R, Liu X, Zhang J, Liu J, Lu Y et al. Mesenchymal stromal cells protect hepatocytes from lipotoxicity through alleviation of endoplasmic reticulum stress by restoring SERCA activity. J Cell Mol Med. 2021;25(6):2976-93.
34. Hu J, Han H, Lau MY, Lee H, MacVeigh-Aloni M, Ji C. Effects of combined alcohol and anti-HIV drugs on cellular stress responses in primary hepatocytes and hepatic stellate and kupffer cells. Alcohol Clin Exp Res. 2015;39(1):11-20.
35. Wang H, Han B, Wang N, Lu Y, Gao T, Qu Z, Yang H, Yang Q. Oxymatrine attenuates arsenic-induced endoplasmic reticulum stress and calcium dyshomeostasis in hepatic stellate cells. Ann Transl Med. 2020;8(18):1171.
36. Cai SY, Ouyang X, Chen Y, Soroka CJ, Wang J, Mennone A, Wang Y, Mehal WZ, Jain D, Boyer JL. Bile acids initiate cholestatic liver injury by triggering a hepatocyte-specific inflammatory response. JCI Insight. 2017;2(5):e90780.
37. Bochkis IM, Rubins NE, White P, Furth EE, Friedman JR, Kaestner KH. Hepatocyte-specific ablation of Foxa2 alters bile acid homeostasis and results in endoplasmic reticulum stress. Nat Med. 2008;14(8):828-36.
38. Kim JY, Choi JH, Kim SH, Park H, Lee D, Kim GJ. Efficacy of Gene Modification in Placenta-Derived Mesenchymal Stem Cells Based on Nonviral Electroporation. Int J Stem Cells. 2021;14(1):112-18.
39. Kim JY, Park S, Lee HJ, Lew H, Kim GJ. Functionally enhanced placenta-derived mesenchymal stem cells inhibit adipogenesis in orbital fibroblasts with Graves' ophthalmopathy. Stem Cell Res Ther. 2020;11(1):469.
40. Zhang X, Zhang K. Endoplasmic Reticulum Stress-Associated Lipid Droplet Formation and Type II Diabetes. Biochem Res Int. 2012;2012:247275.
41. Brewer JW, Diehl JA. PERK mediates cell-cycle exit during the mammalian unfolded protein response. Proc Natl Acad Sci U S A. 2000;97(23):12625-30.
42. Pallen CJ, Valentine KA, Wang JH, Hollenberg MD. Calcineurin-mediated dephosphorylation of the human placental membrane receptor for epidermal growth factor urogastrone. Biochemistry. 1985;24(18):4727-30.
43. Sanchez-Gonzalez P, Jellali K, Villalobo A. Calmodulin-mediated regulation of the epidermal growth factor receptor. FEBS J. 2010;277(2):327-42.
44. Rachakhom W, Khaw-On P, Pompimon W, Banjerdpongchai R. Dihydrochalcone Derivative Induces Breast Cancer Cell Apoptosis via Intrinsic, Extrinsic, and ER Stress Pathways but Abolishes EGFR/MAPK Pathway. Biomed Res Int. 2019;2019:7298539.

Figures

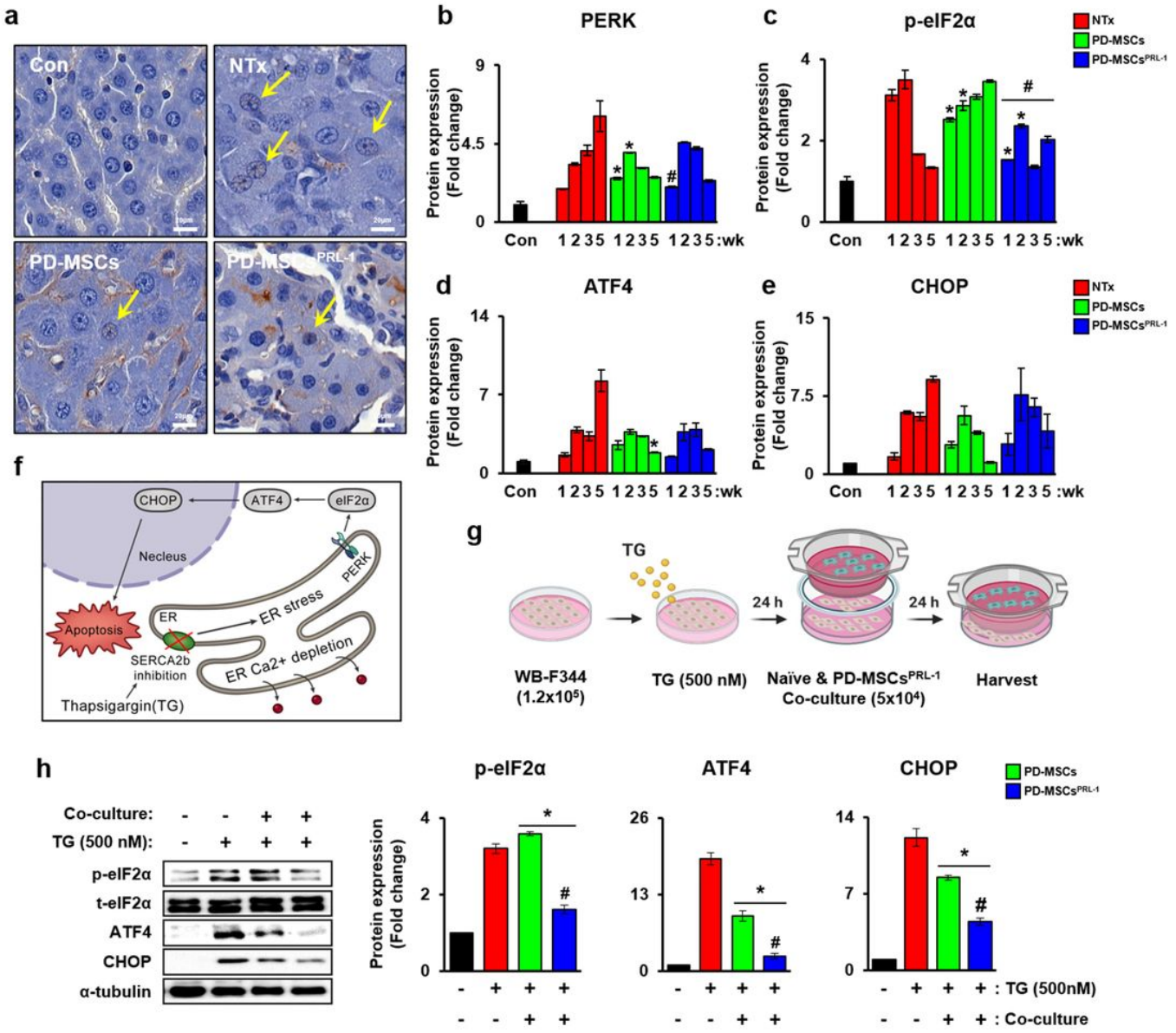

Figure 1

PD-MSCPRL-1 transplantation decreased ER stress in a rat model with BDL and in hepatocytes. a Representative IF images of CHOP in cirrhotic livers at 5 weeks by IHC. b-e Quantification of ER stress markers (e.g., PERK, total and phosphorylated eIF2 alpha; p-eIF2α, ATF4, and CHOP) by PD-MSCPRL-1 transplantation in pooled BDL-injured rat liver protein (n = 5/group) at 1, 2, 3, and 5 weeks. f A schematic diagram showing ER stress induced by TG. g A schematic diagram describing the TG (500 nM)-treated WB-F344 cells cocultivated with PD-MSC or PD-MSCPRL-1 for 24 h. h Western blotting and i the intensities of ER stress markers in WB-F344 cells. α-tubulin was used as loading control. Data from each group are shown as the mean ± SD, assessed by Student's t-test. *p < 0.05 vs NTx, #p < 0.05 vs PD-MSCs.

ATF4, activating transcription factor 4; BDL, bile duct ligation; CHOP, C/EBP homologous protein; p-eIF2α, phosphorylated eIF2 alpha; PRL-1, phosphatase of regenerating liver-1; TG, thapsigargin

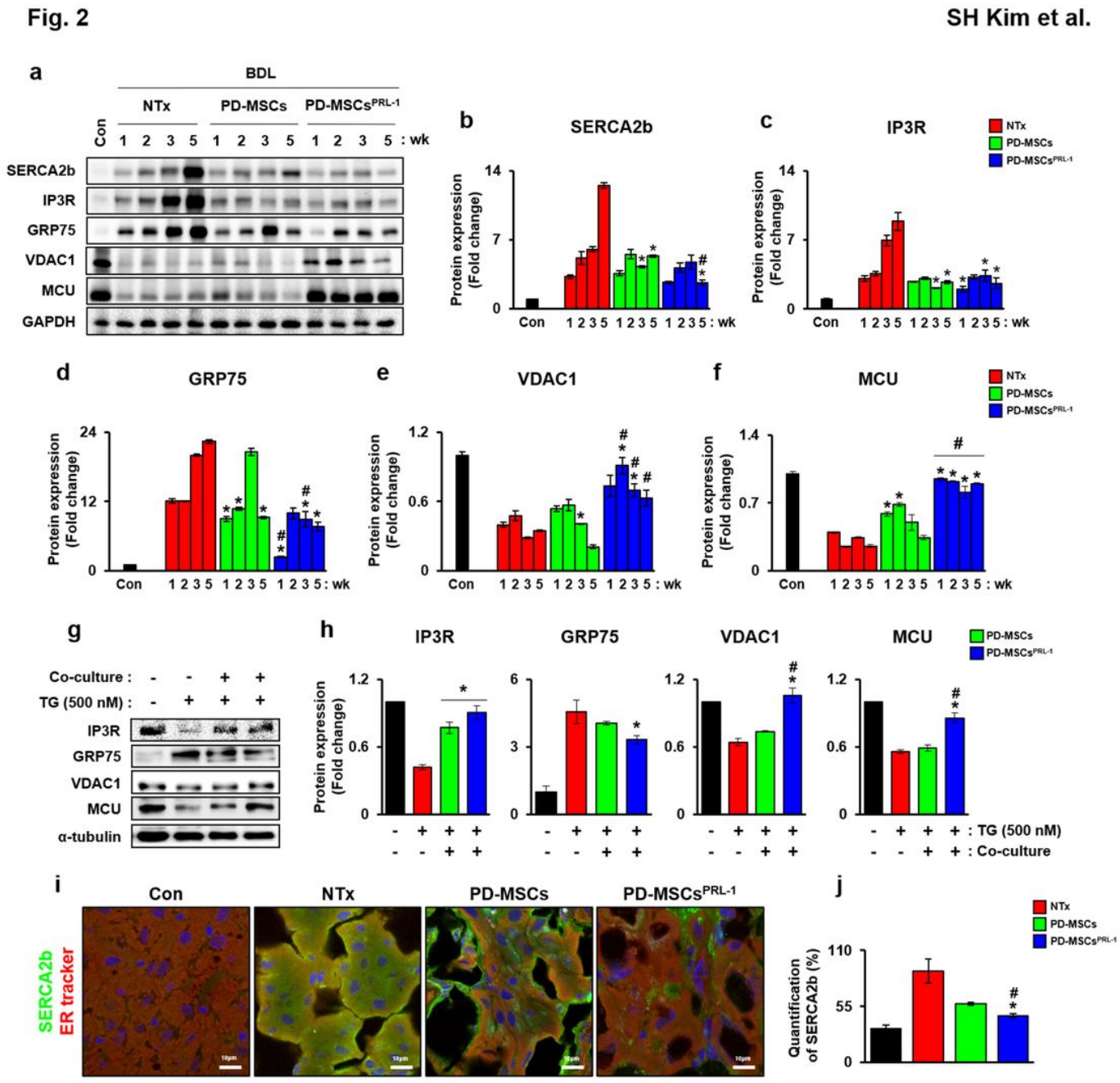

Figure 2

PD-MSCPRL-1 transplantation regulated calcium channels in a rat model of BDL and in hepatocytes. a Western blotting and b-f the intensities of calcium channels (e.g., SERCA2b, IP3R, glucose regulated protein 75; GRP75, voltage dependent anion channel 1; VDAC1, and mitochondria calcium uniporter; MCU) by PD-MSCPRL-1 transplantation in BDL-induced rat liver protein measured using glycraldehyde-3-

phosphate dehydrogenase (GAPDH) as loading control. g Western blotting and h the intensities of calcium channels (e.g., IP3R, GRP75, VDAC1, MCU, and CaM) in TG (500 nM)-treated WB-F344 cells cocultivated with PD-MSCs or PD-MSCsPRL-1 for 24 h. α-Tubulin was used as a loading control. i Representative images and j quantification of SERCA2b (green) and ER Tracker (red) in BDL-injured rat livers at 5 weeks by IF staining. DAPI (blue) was used for counterstaining. Data from each group are shown as the mean ± SD, assessed by Student's t-test. *p < 0.05 vs NTx, #p < 0.05 vs PD-MSCs. BDL, bile duct ligation; CaM, Calmodulin; GAPDH, glycraldehyde-3-phosphate dehydrogenase; GRP75, glucose regulated protein 75; IP3R, inositol trisphosphate receptor; MCU, mitochondria calcium uniporter; NTx, nontransplantation; PRL-1, phosphatase of regenerating liver-1; SERCA2b, sarco/endoplasmic reticulum Ca2+ ATPase; VDAC1, voltage dependent anion channel 1

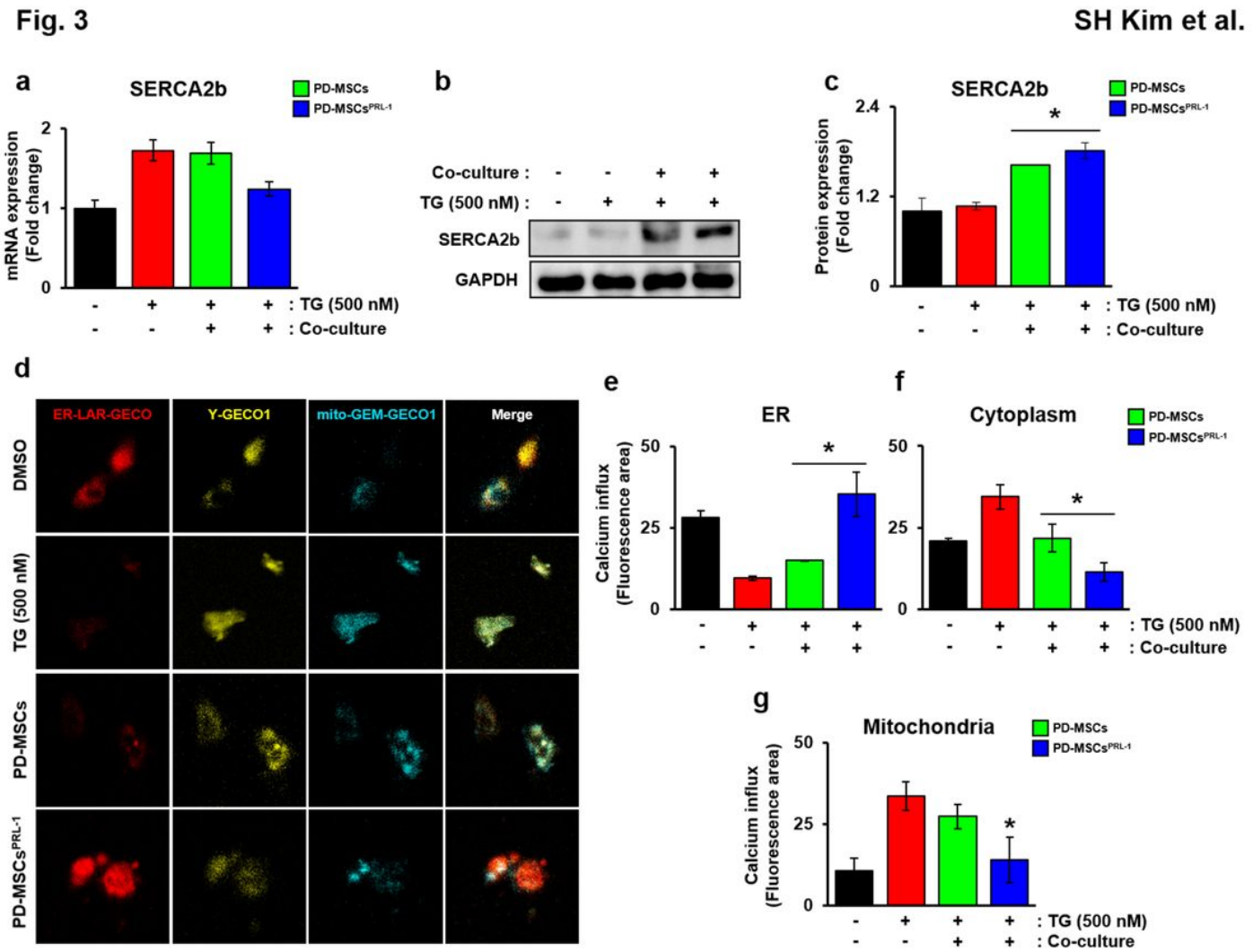

Figure 3

PD-MSCsPRL-1 regulated calcium influx in rat hepatocytes. a mRNA and b, c protein levels of SERCA2b in the TG (500 nM)-treated WB-F344 cells cocultured with PD-MSCs or PD-MSCPRL-1 for 24 h. GAPDH was

used as a loading control. d Representative fluorescence images and e-g the fluorescence intensities of calcium influx using ER-LAR GEGO for ER (red), Y-GECO1 for cytoplasm (yellow), and mt-GEM-GECO1 for mitochondria (cyan blue) in the TG (500 nM)-treated WB-F344 cells cocultivated with PD-MSCs or PD-MSCsPRL-1 for 24 h. Data from each group are shown as the mean ± SD, assessed by Student's t-test. *p < 0.05 vs NTx, #p < 0.05 vs PD-MSCs. GAPDH, glycraldehyde-3-phosphate dehydrogenase; NTx, nontransplantation; PRL-1, phosphatase of regenerating liver-1; SERCA2b, sarco/endoplasmic reticulum Ca2+ ATPase; TG, thapsigargin

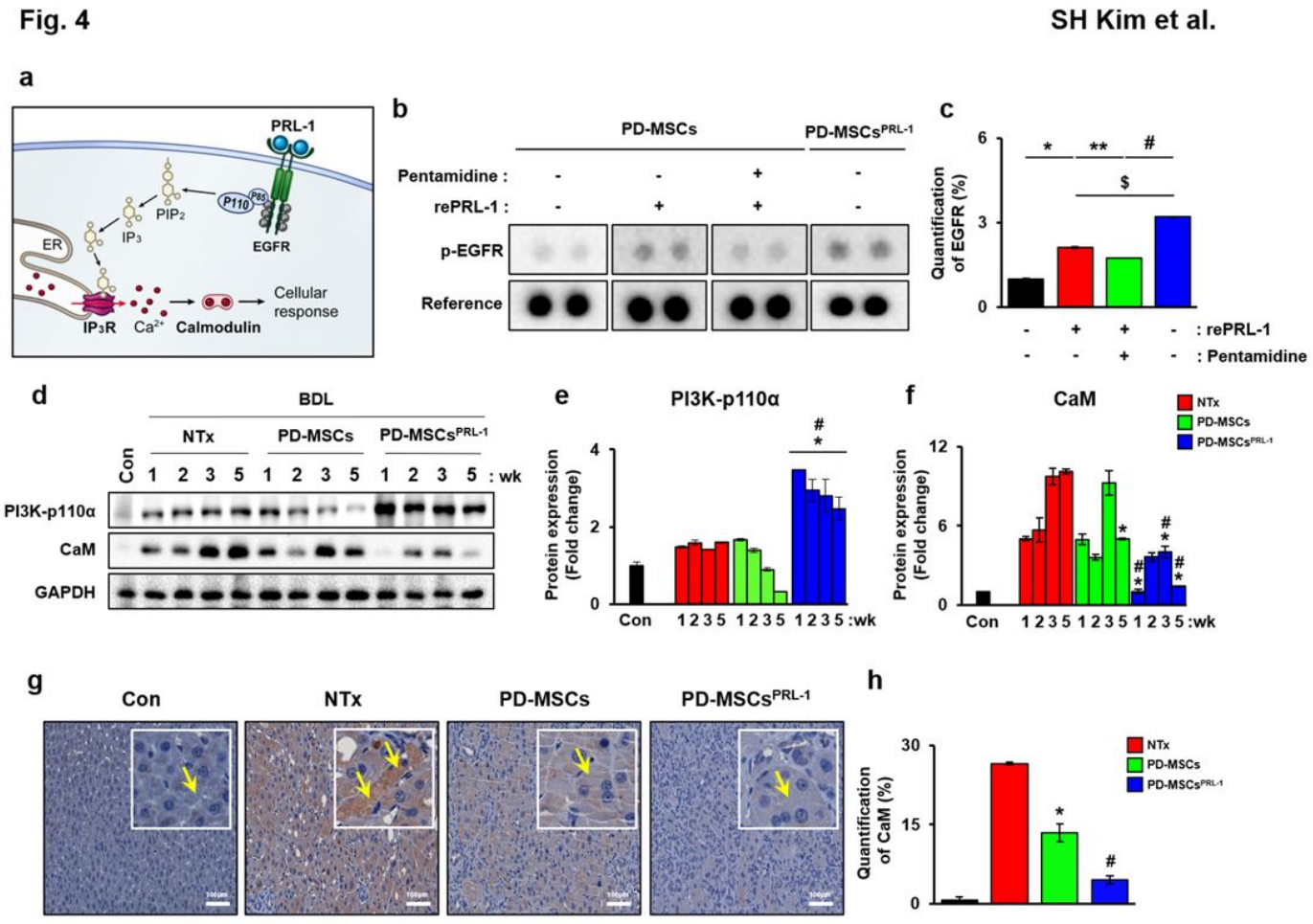

Figure 4

PRL-1 regulated calcium channels by EGFR-PI3K-CaM calcium signaling in BDL-injured rat liver. a A schematic diagram showing the effects of PRL-1 through EGFR and downstream factors (e.g., IP3R and CaM). b Dot blots and c their intensities by phosphorylated RTK assays; *p < 0.05 vs PD-MSCs, **p < 0.05 vs PD-MSCs with recombinant PRL-1 (rePRL-1), #p < 0.05 vs PD-MSCs with rePRL-1 and pentamidine, $p < 0.05 vs PD-MSCs with rePRL-1. d Western blotting and e and f the intensities of PI3K-p110α and CaM in BDL-induced rat livers. GAPDH was used as a loading control. g CaM expression and h its positive area in BDL-induced rat liver by IHC. Data from each group are shown as the mean ± SD, assessed by Student's t-

test. *p < 0.05 vs NTx, #p < 0.05 vs PD-MSCs. BDL, bile duct ligation; CaM, calmodulin; EGFR, epidermal growth factor receptor; GAPDH, glycraldehyde-3-phosphate dehydrogenase; IP3R, inositol trisphosphate receptor; NTx, nontransplantation; PI3K, phosphatidylinositol-3-kinase; PRL-1, phosphatase of regenerating liver-1; RTK, receptor tyrosine kinase

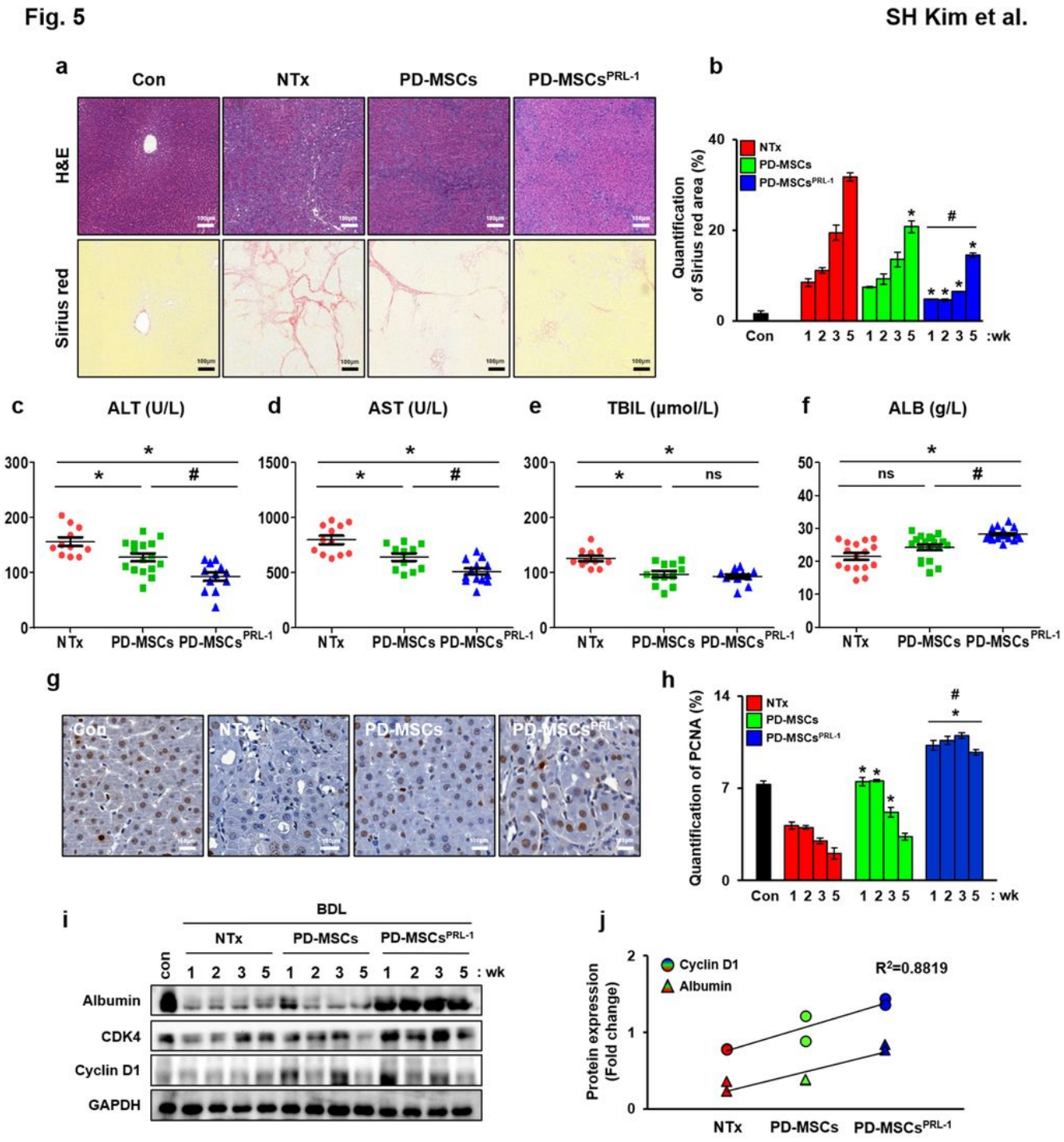

Figure 5

Hepatic regenerative effects of PD-MSCsPRL-1 in a rat model of BDL. a Representative images of histological analysis of BDL rat liver sections by H&E and Sirius red staining. b Quantification of Sirius red positive area. c-f Serological analysis of ALT, AST, TBIL, and ALB in individual rat serum (n = 20/group). g PCNA expression and h quantification of the PCNA-positive area in a rat liver section from each group determined by IHC. i Western blotting of liver regeneration markers (e.g., ALB, CDK4, and cyclin D1) in BDL-induced rat liver protein. GAPDH was used as loading control. j Positive correlation value between ALB and cyclin D1. Data from each group are shown as the mean ± SD, assessed by Student's t-test or one-way ANOVA. *p < 0.05 vs NTx, #p < 0.05 vs PD-MSCs. ALT, alanine aminotransferase; ALB, albumin; AST, aspartate aminotransferase; BDL, bile duct ligation; CDK4, cyclin-dependent kinase 4; GAPDH, glycraldehyde-3-phosphate dehydrogenase; NTx, nontransplantation; PCNA, proliferating cell nuclear antigen; PRL-1, phosphatase of regenerating liver-1; TBIL, total bilirubin

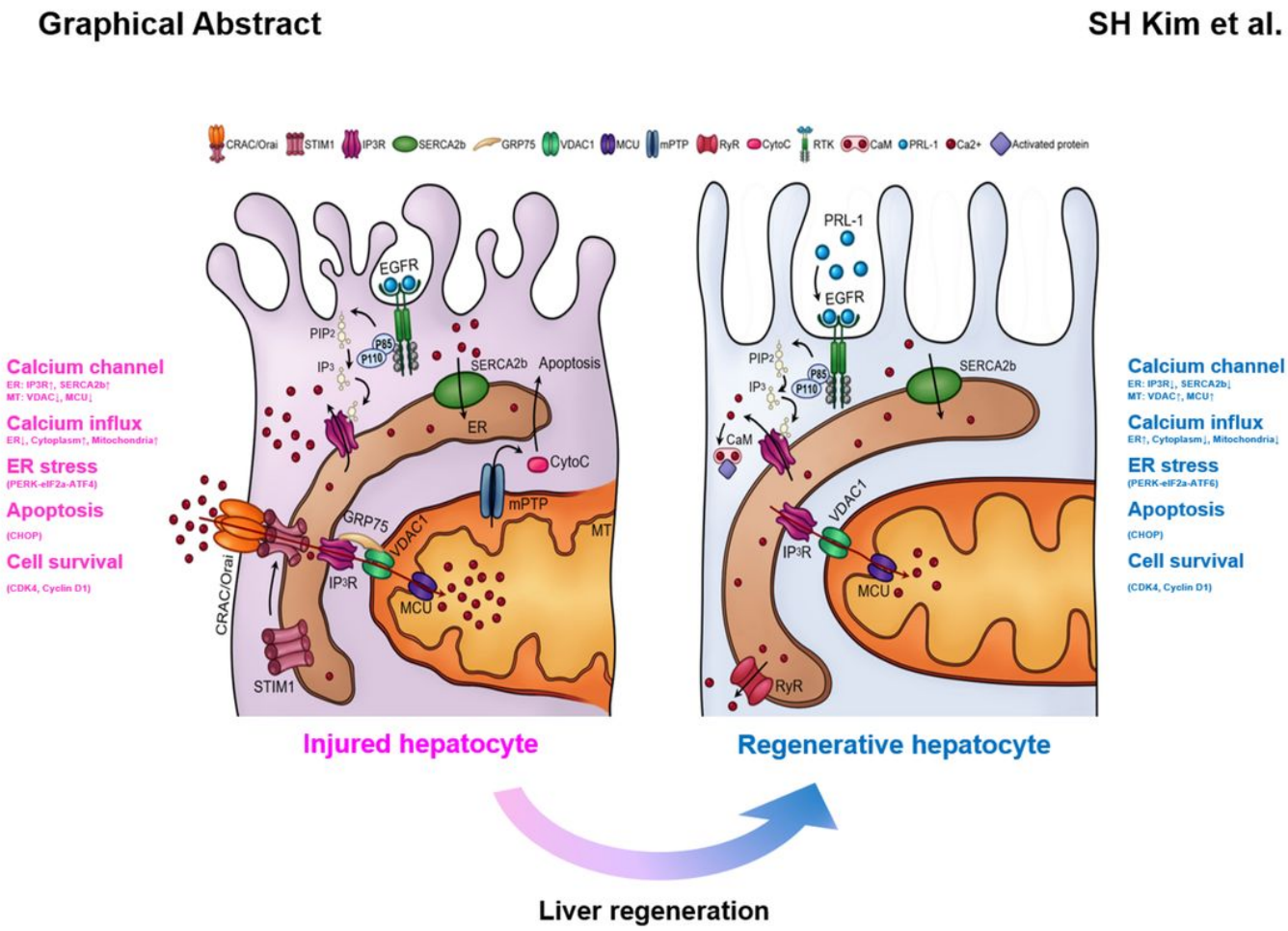

Figure 6

Graphical abstract describing improved hepatic functions and decreased ER stress and calcium influx by PD-MSCPRL-1 transplantation in hepatocytes from a rat BDL model through the EGFR-PI3K-CaM

signaling pathway. BDL, bile duct ligation; CaM, calmodulin; EGFR, epidermal growth factor receptor; PRL-1, phosphatase of regenerating liver-1; PI3K, phosphatidylinositol-3-kinase

Supplementary Files

This is a list of supplementary files associated with this preprint. Click to download.

- SCRTSupportinginformationKimetal.doc
- SupplementaryTableSHKimfinal.doc